Journal of Power Sources 196 (2011) 7806–7811

Contents lists available at ScienceDirect

Journal of Power Sources

journal homepage: www.elsevier.com/locate/jpowsour

Short communication

Designing current collector/composite electrode interfacial structure of organic radical battery

Sunao Yoshihara[a,b], Haruhiko Katsuta[a], Hiroshi Isozumi[a], Masanori Kasai[a], Kenichi Oyaizu[b], Hiroyuki Nishide[b,*]

[a] DP Development Center, DIC Corporation, Tokyo 174-8520, Japan
[b] Department of Applied Chemistry, Waseda University, Tokyo 169-8555, Japan

ARTICLE INFO

Article history:
Received 27 September 2010
Accepted 28 October 2010
Available online 3 November 2010

Keywords:
Secondary battery
Radical polymer
Composite electrode
Charging–discharging characteristics

ABSTRACT

Charge/discharge processes of organic radical batteries based on the radical polymer's redox reaction should be largely influenced by the structure and the composition of the composite electrodes. AC impedance measurement of the composite electrodes reveals a strong correlation between the overall electron transfer resistance of the composite electrode and the material of the current collector, and suggests that the electric conduction to the current collector through the contact resistance should be crucial. We also find that the adhesion and the contact area between the composite electrode and the current collector strongly influence the contact resistance rather than the work functions and the volume resistivities of the composite electrode and the current collector. It is also confirmed that the charge/discharge performance of the composite electrode is related to the overall electron transfer resistance of the composite electrode. These results indicate that the charge/discharge performance of the radical battery is dominated by the interfacial electron transfer processes at the current collector/carbon fiber interface. In fact, the composite electrode which has a high adhesion to the current collector shows a small overall electron transfer resistance and an excellent charge/discharge performance. The rate performance would be much improved by suitably designing the interfacial structure including adhesion and contact area.

1. Introduction

Recently, organic polymers with redox-active and chemically stable radical pendant substituents are attracting much attention due to its specific characteristics based on their rapid and repeatable oxidation/reduction capabilities [1–6]. The typical example of the pendant substituents in the so-called radical polymers is the 2,2,6,6-tetramethylpiperidinyl-*N*-oxy (TEMPO) groups, which is sufficiently robust as well as rapidly, reversibly, and stoichiometrically oxidized to the corresponding oxoammonium cation via chemical or electrochemical oxidation. Studies on the redox chemistry of the radical polymers have been encouraged by our recent approach to the "radical battery" [7–15], which is characterized by an excellent rate performance and potential capability of fabricating purely organic, paper-like, and flexible rechargeable energy-storage devices. A schematic of the radical battery structure and the mechanism of charge/discharge processes of the battery are shown in Scheme 1. Radical batteries are featured by the use of the radical polymers as the cathode-active materials, together with anode-active materials such as Li metal sandwiching an electrolyte layer. The typical cathode consists of the radical polymer, a carbon fiber as the conductive additive, and a small amount of binders to enhance adhesion to current collectors. The charge/discharge processes of the batteries are based on the radical polymer's redox reaction. The carbon fibers work as the electric conduction path to assist the repeatable oxidation/reduction processes throughout the radical polymer layer. The structure and composition of the radical polymer/carbon fiber composite electrode are thus one of the most important factors and determine the overall characteristics of the radical battery. We supposed that determination of the factor, most responsible for the overall electron transfer reactions, is the shortcut to improve the battery performance. In this paper, we report the electrochemical analysis on the radical polymer/carbon fiber composite electrodes with a view to unravel the most influential factor for the overall charge/discharge process, focusing on the electron transfer resistance [16–18] obtained from impedance spectroscopy. We demonstrate that the charge/discharge properties of the composite electrode are dramatically improved by modifying the interfacial structure that is one of the most important factors. These results provide a design principle to fabricate radical batteries with excellent performances.

* Corresponding author. Tel.: +81 3 3200 2669; fax: +81 3 3209 5522.
E-mail address: nishide@waseda.jp (H. Nishide).

0378-7753/$ – see front matter © 2010 Elsevier B.V. All rights reserved.
doi:10.1016/j.jpowsour.2010.10.092

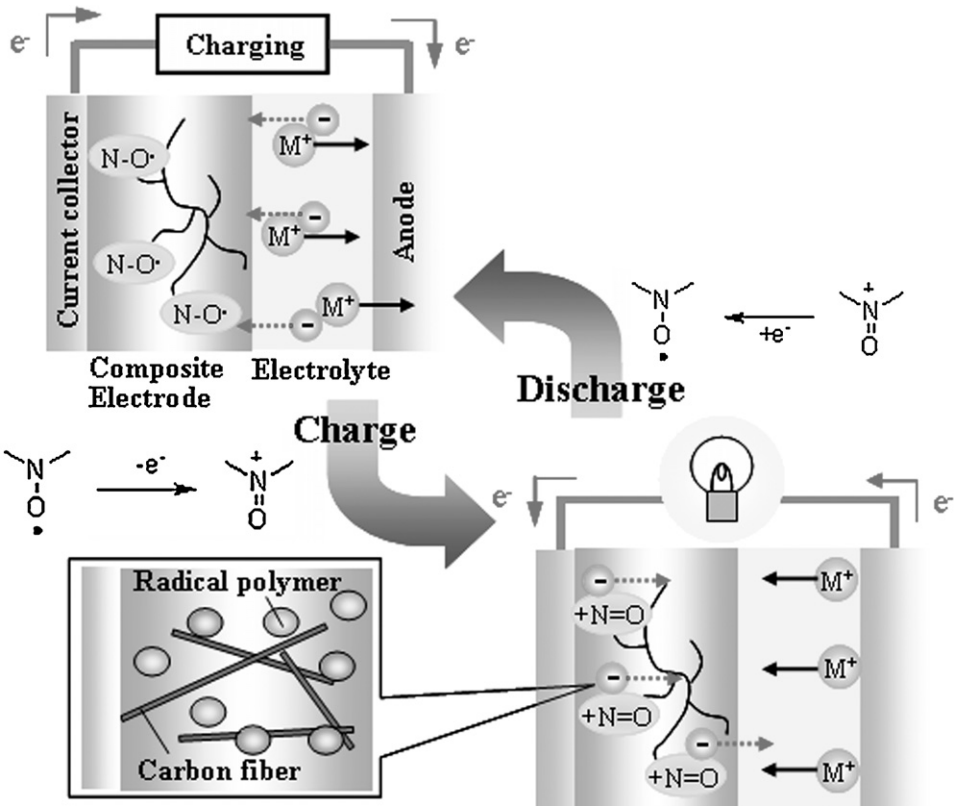

Scheme 1. Charge/discharge mechanism of the radical battery.

2. Experimental

2.1. Materials

All solvents were purchased from Kishida Kagaku Co. Poly(1-oxy-2,2,6,6-tetramethylpiperidin-4-yl vinyl ether) (PTVE), the radical polymer employed as the electrode-active material in this report, was prepared as described previously by our group [19–21]. A vapor-grown carbon nanofiber (VGCF-H) was purchased from Shouwa Denko Co. Poly(vinylidene fluoride) (PVdF) resin (KF#1300), employed as a binder resin in an *N*-methyl-2-pyrrolidone (NMP) based ink (i.e. a dispersion of the polymer/carbon nanofiber), was purchased from Kureha Chemical Co. An electrochemical grade solution of 1 M lithium bis(pentafluoroethanesulfonyl)imide (LiBETI) in propylene carbonate (PC) was purchased from Kishida Kagaku Co. All materials were used without further purification.

2.2. Preparation of composite electrodes

The radical polymer/carbon fiber composite electrodes were prepared on current collectors using several kinds of inks by stencil printing process. We prepared several compositions of NMP-based inks for our experiment. The preparative method for the composite electrodes from the NMP-based inks was as follows. A radical polymer, PTVE, was mixed with VGCF-H and PVdF in NMP by a relatively low-powered disperser to obtain the NMP-based inks. Nonvolatile content of each NMP-based ink was adjusted to 10%. The obtained inks were stencil printed with a contact metal mask to give wet films with thickness around 180 μm on various substrates (i.e. current collectors such as an ITO/glass plate, a platinum plate, and a glassy carbon plate), and then dried under vacuum at 80 °C for 12 h to give several kinds of the composite electrodes of the same size ($A = 1\ cm^2$) and thickness (about 20 μm) with varied composition, PTVE/VGCF-H/PVdF = 10/80/10, 30/60/10, 50/40/10, and 70/20/10 (w/w/w). Hereinafter NMP-based inks with compositions of PTVE/VGCF-H/PVdF = 10/80/10, 30/60/10, 50/40/10, and 70/20/10 (w/w/w) are abbreviated as N1, N2, N3, and N4, respectively. Thicker films of the composite electrodes were obtained similarly by using the corresponding thicker metal masks. A SEM image of a composite electrode was obtained without any deposition using a 3D real surface view microscope (VE-9800/Keyence Co.). The SEM image of the composite electrode prepared from N1 (Fig. 1) showed a typical network of the carbon fibers and the radical polymer was situated within the carbon network. The carbon fiber network provide a conducting path which allows the repeatable redox processes of the radical polymer, and the redox efficiency of

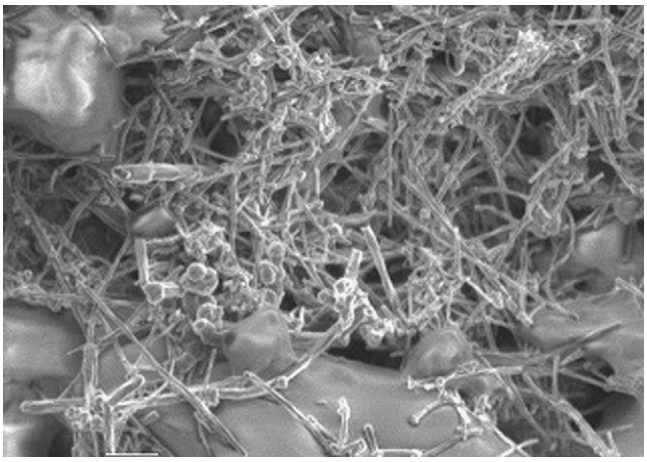

Fig. 1. SEM image (5000×) of the composite electrode prepared from N1. The fibrous network corresponds to the carbon fiber, and the clayey particle corresponds to the radical polymer.

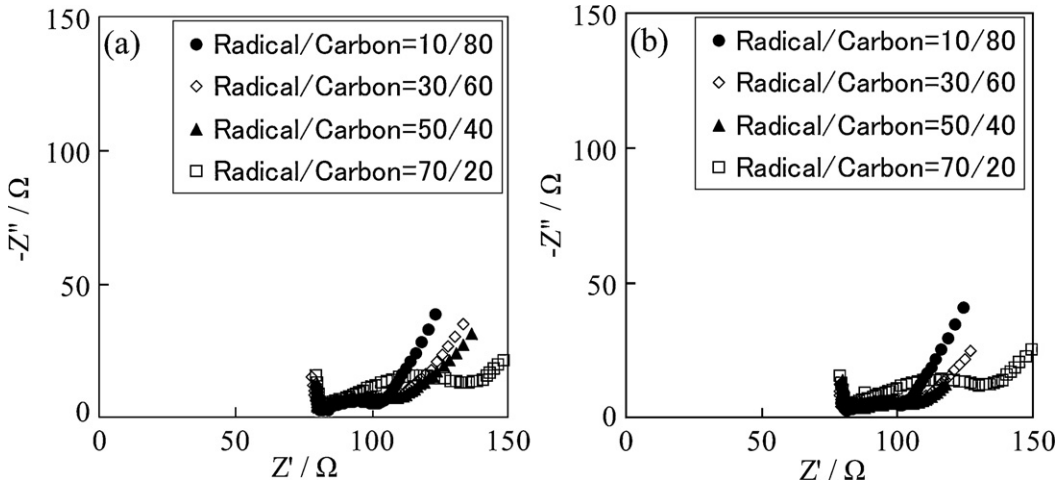

Fig. 2. Nyquist plots of several composite electrodes prepared from N1, N2, N3, and N4. The dry film thicknesses of the composite electrodes measured in (a) and (b) were about 20 μm and 60 μm, respectively (film thicknesses of the composite electrodes measured in (b) were three times the thicknesses of those measured in (a)). Current collectors of all the composite electrodes were glassy carbon plates. Enlarged spectra are shown as insets.

the composite electrode depends on the degree of dispersion of the carbon fiber and the radical polymer.

2.3. Electrochemical measurements of composite electrodes

Electrochemical measurements such as AC impedance spectroscopy and charging/discharging experiments of the composite electrodes were carried out in a conventional three-electrode cell using a 1287 type potentiostat–galvanostat and a 1255WB type electrochemistry measurement system (Solartron). All experiments were carried out at 25 °C (vide infra). Platinum wire and commercial Ag/Ag^+ immersed in a solution of 0.01 M $AgNO_3$ and 0.1 M tetrabutylammonium perchlorate (TBAP) in CH_3CN were used as the auxiliary electrode and the reference electrode, respectively. These electrodes were purchased from BAS Co. Composite electrodes with various compositions, prepared on various current collectors, were used as the working electrode. In AC impedance measurements, the frequency range was 10^5 to 10^{-2} Hz with an AC amplitude of 10 mV. The DC bias voltage was set at $(E_{pa} + E_{pc})/2$ of each cells, at which 50% of the nitroxide radical units in the polymer were supposed to be oxidized to the cationic state (i.e. the oxoammonium cation).

3. Results and discussion

3.1. AC impedance measurements of composite electrodes

The structures and the properties of the composite electrodes including the current collector are one of the most important factors that influence on the overall characteristics of the battery, because the charge/discharge processes of the batteries involve the radical polymer's redox reaction in the composite electrodes. To elucidate the electron transfer resistances (including the charge transfer resistance) of the composite electrodes, which would have a correlation with the structure and the properties of the composite electrodes, AC impedance analysis of the composite electrodes were investigated. AC impedance measurement is more commonly used to elucidate the electron transfer resistance of various composite materials, for example, the hydrogen evolution reaction in fuel cells [22] and the electrochemical properties of anodes in lithium ion batteries [23,24]. In Nyquist plots, the *x*- and the *y*-axis represent the real (Z') and the imaginary part (Z'') of the impedance spectra, respectively. Fig. 2 shows the impedance spectra obtained for the three-electrode cell, in which the composite electrode, a platinum wire, and the Ag/Ag^+ electrode are used as the working, the auxiliary, and the reference electrodes, respectively. Typical semicircle-shaped impedance spectra were observed showing the real-axis intercepts at the low-frequency region corresponding to the resistance of the electrolyte solution (R_s) and at the high-frequency region corresponding to the resistance of the three-electrode cell (R). And the difference in the value of R_s and R were assumed to be R_f (the resistance of composite electrode including the charge transfer resistance and the composite electrode/current collector interfacial resistance). When the Nyquist plot has only one real-axis intercept (R_s is equal to R), R_f value is nearly equal to zero. Remarkably, R_s values were nearly constant (between 70 and 80 Ω) in all impedance spectra of the composite electrodes examined in the present study, which suggested that the propylene carbonate solution of 1 M LiBETI used in the impedance measurement had sufficiently high ionic conductivity of the lithium cation. The Nyquist plots for the composite electrodes on glassy carbon plates prepared from the NMP-based ink showed that R_f values became larger as the composition of the radical polymer increased (i.e., as the carbon fiber content decreased) and was little influenced by the thicknesses of the composite electrodes (Fig. 2, Table 1). It was indicated that R_f values was influenced by the composition of the compos-

Table 1
The resistance data (R_s, R, and R_f) calculated from Nyquist plot described in Fig. 2.

Entry	Figure	Radical polymer (%)	Carbon fibre (%)	Thickness (μm)	R_s (Ω)	R (Ω)	R_f (Ω)
1	Fig. 2(a)	10	80	20	82	102	20
2		30	60		82	103	21
3		50	40		81	106	25
4		70	20		83	133	50
5	Fig. 2(a)	10	80	60	81	101	20
6		30	60		81	104	23
7		50	40		84	106	22
8		70	20		82	130	48

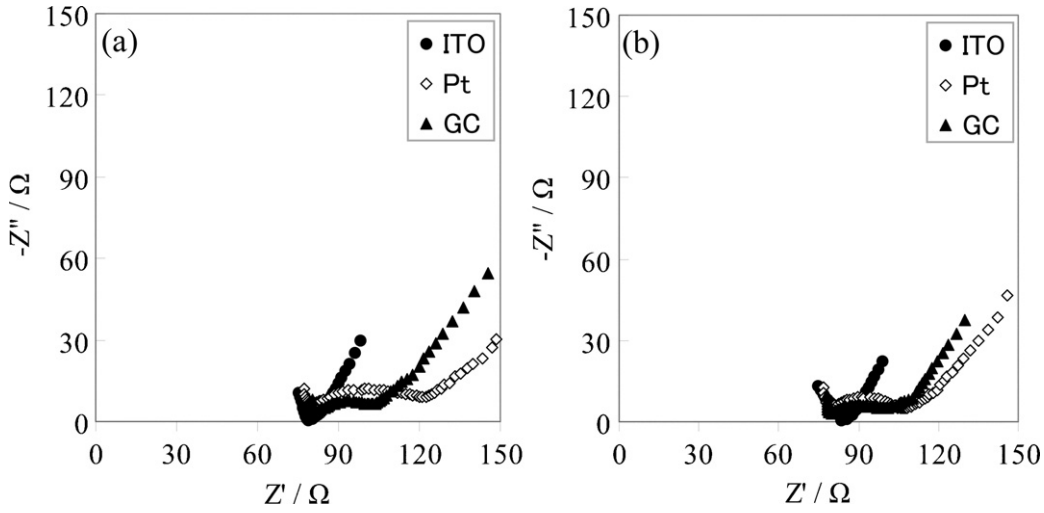

Fig. 3. Nyquist plots of composite electrodes on various current collectors of an ITO/glass plate, a glassy carbon plate, and a platinum plate. Composite electrodes were prepared from (a) N1, (b) N3. The dry film thicknesses of the composite electrodes were about 20 μm.

ite electrode, which would change the contact resistances between the composite electrodes and the current collectors.

3.2. AC impedance measurements of composite electrodes on the different current collectors

The impedance spectra of composite electrodes prepared on various current collectors such as an ITO/glass plate, a platinum plate, and a glassy carbon plate were shown in Fig. 3. The R_f values obtained in the impedance spectra of the composite electrodes prepared from N1 and N3 depended on the current collectors. The composite electrodes on the ITO/glass plates gave smaller R_f values than those on the platinum plates and the glassy carbon plates. The composite electrodes prepared from N1 gave larger R_f values on a platinum plate than those on a glassy carbon plate. However, the composite electrodes prepared from N3 gave a small difference of R_f values on a glassy carbon plate and on a platinum plate. These results suggested that R_f value was strongly influenced by a combination of the material of current collector and the composition of the composite electrode, which would influence the carbon fiber/current collector interface contact resistance.

3.3. Charging–discharging characteristics of the composite electrodes on the different current collectors

The difference in the R_f values of the composite electrodes would reflect in the charging/discharging behavior, especially for those prepared from N1 on an ITO/glass plate and those on a glassy carbon plate. To examine the influence of R_f to the charge/discharge properties, the charge/discharge experiments of those two composite electrodes were carried out (Fig. 4). A distinct effect of R_f on the charge/discharge properties was observed for these composite electrodes even with the identical compositions. The charge/discharge experiments of the composite electrode by the constant current electrolysis revealed that a specific capacity obtained with an ITO/glass plate as the current collector was larger than that with a glassy carbon plate. These results suggested that the charge/discharge properties of the composite electrodes were strongly related to R_f values of the composite electrodes observed in the Nyquist plots. The composite electrode with the small R_f showed a remarkably excellent charge/discharge property.

3.4. Superiority of the ITO/glass current collector

Work functions of an ITO/glass plate, a glassy carbon plate, a platinum plate, and the several compositions of composite electrodes were measured by a UPS spectrometer (Model AC-1/Riken Keiki Co., Ltd.) with an ambient ultraviolet photoelectron spectroscopy (UPS) technique. Observed work functions and theoretical volume resistivities of an ITO/glass plate, a glassy carbon plate, and a platinum plate, and observed work functions of the composite electrodes were described in Table 2. The work function datum revealed that the energy barrier between an ITO/glass plate and the composite electrodes was higher than that between a platinum plate and the composite electrodes. And the theoretical volume resistivities revealed that electrons could transfer in a platinum plate more smoothly than in an ITO/glass plate. These results could not explain that the composite electrode on an ITO/glass plate had shown the minimum overall resistance. AC impedance of the composite electrodes with different adhesions (with different contact

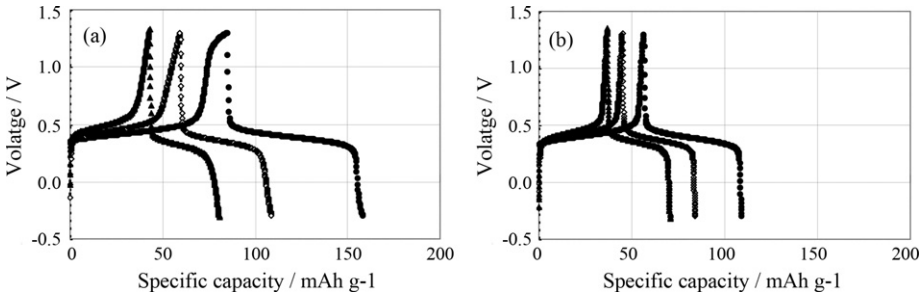

Fig. 4. Charge/discharge curves of the composite electrodes prepared from N1 on various current collectors of (a) an ITO/glass plate, and (b) a glassy carbon plate. Charging–discharging rate were 1 C, 5 C, and 10 C, respectively.

Table 2
Work functions and volume resistivites of an ITO/glass plate, a glassy carbon plate, a platinum plate, and composite electrodes.

	ITO/glass plate	Glassy carbon plate	Platinum plate	Composite electrode
Volume resistivity (Ω cm)	1.0E – 04	4.5E – 03	1.0E – 05	–
Work function (eV)	4.9	4.9	5.4	5.5–5.8

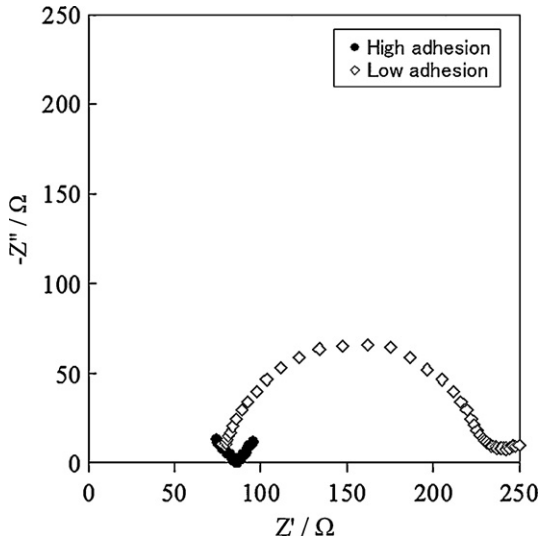

Fig. 5. Nyquist plots of composite electrodes with a low adhesion and a high adhesion to an ITO/glass plate prepared from N3 on an ITO/glass plate. The dry film thicknesses of the composite electrodes were about 20 μm

areas) to an ITO/glass plate was measured (Fig. 5). R_f value of the composite electrode which had a low adhesion (had a small contact area) to an ITO/glass plate was larger than that had a high adhesion (had a large contact area) to an ITO/glass plate, even with the identical composition and the same current collector. The composite electrode which had a low adhesion (had a small contact area) was made as follow. The composite electrode made on the release seat was peeled off and put on an ITO/glass. Spraying process (spray some NMP to the composite electrode laid on an ITO/glass) and drying process provided the composite electrode with a low adhesion (with a small contact area). A difference in the adhesion of the composite electrode to an ITO/glass was evaluated using adhesion strength test (ISO-2409). In the adhesion strength test (ISO-2409), 10×10 (1^2 mm) cross-cut composite electrode on the current collector was peeled off by the cellophane adhesive tape and the adhesion is evaluated from the amount of fragments of the cross-cut composite electrode bonded to the cellophane adhesive tape. If 15–35% of fragments were bonded to the tape, the adhesion was classified into Class 3, and if over the 65% of fragments were bonded to the tape, the adhesion was classified into Class 5. Degrees of adhesion of the composite electrodes which had a low adhesion to an ITO/glass plate and a high adhesion to an ITO/glass plate were classified into class 5 and class 3, respectively. Degrees of adhesion of the composite electrodes on a platinum plate and on a glassy carbon plate prepared from N3, which were described in Section 3.2 and had larger R_f values than the composite electrode on a ITO/glass plate, were classified into Class 5. Thus we assumed that the superiority of an ITO/glass plate as a current collector material would be originated by the adhesion and the contact area to the composite layers (depending on the surface roughness, etc.), rather than their work functions and volume resistivities. Some researchers also focused on the adhesion between conductive materials and current collectors, and reported that the adhesion influences the properties of conductive material/current collector composites [25,26]. Further study about clarification of the correlation between the adhesion (the contact area) of the composite electrode to the current collector and the R_f value will be the topics of our future work.

4. Conclusion

Charging and discharging properties of the radical polymer/carbon fiber composite electrodes was investigated by focusing on the electron transfer processes. To determine the most effective factor in the composite electrodes, the impedance analysis of the electrodes were investigated. It was revealed that the electric conduction to the current collector through the contact resistance was responsible to dominate the overall electron transfer process, based on the strong correlation between the overall resistance of the composite electrodes including the current collectors and the material of the current collector. The superiority of an ITO/glass plate as a current collector material would be originated by the adhesion to the composite layers and the contact area to the composite layers (depending on the surface roughness etc.), rather than their work functions and volume resistivities. We also confirmed that the charge/discharge performance of the composite electrode was related to the overall electron transfer resistance of the composite electrode including the current collectors. These results suggested that the charge/discharge performance of the organic radical battery was dominated by the interfacial electron transfer processes at the current collector/carbon fiber interface. A better performance of the battery is expected with electrode-active materials which accomplishes a closer contact of the current collector and the composite electrode. Further studies on the electron transfer process between the current collector and the composite electrode are continued to improve the organic radical battery characteristics.

Acknowledgements

This work was partially supported by the NEDO Project on "Radical Battery for Ubiquitous Power". The authors appreciate the discussion with Fundamental and Environmental Research Laboratory, NEC Co. and Functional Chemicals Research Laboratory, Sumitomo Seika Chemicals Co. This work was carried out at the DP Development Center, DIC Co. and the Advanced Research Institute for Science & Engineering, Waseda University.

References

[1] C.A. McNamara, M.J. Dixon, M. Bradley, Chem. Rev. 102 (2002) 3275–3300.
[2] T. Fulghum, P. Taranekar, R. Advincula, Macromolecules 41 (2008) 5681–5687.
[3] H. Kanazawa, M. Higuchi, K. Yamamoto, J. Am. Chem. Soc. 127 (2005) 16404–16405.
[4] P. Novak, K. Muller, K.S.V. Santhanam, O. Haas, Chem. Rev. 97 (1997) 207–282.
[5] A. Dijksman, A. Marino-González, A.M.I. Payeras, I.W.C.E. Arends, R.A. Sheldon, J. Am. Chem. Soc. 123 (2001) 6826–6833.
[6] Y. Yonekuta, K. Oyaizu, H. Nishide, Chem. Lett. 36 (2007) 866–867.
[7] H. Nishide, K. Oyaizu, Science 319 (2008) 737–738.
[8] H. Nishide, T. Suga, Electrochem. Soc. Interface 14 (2005) 32–36.
[9] Y. Yonekuta, K. Susuki, K. Oyaizu, K. Honda, H. Nishide, J. Am. Chem. Soc. 129 (2007) 14128–14129.
[10] K. Koshika, N. Sano, K. Oyaizu, H. Nishide, Chem. Commun. 7 (2009) 836–838.
[11] T. Suga, H. Ohshiro, S. Sugita, K. Oyaizu, H. Nishide, Adv. Mater. 21 (2009) 1627–1630.
[12] K. Koshika, N. Sano, K. Oyaizu, H. Nishide, Macromol. Chem. Phys. 210 (2009) 1989–1995.
[13] K. Oyaizu, H. Nishide, Adv. Mater. 21 (2009) 2339–2344.
[14] K. Nakahara, S. Iwasa, M. Satoh, Y. Morioka, J. Iriyama, M. Suguro, E. Hasegawa, Chem. Phys. Lett. 359 (2002) 351–354.
[15] K. Oyaizu, T. Suga, K. Yoshimura, H. Nishide, Macromolecules 41 (2008) 6646–6652.
[16] K. Nakahara, J. Iriyama, S. Iwasa, M. Suguro, M. Satoh, E.J. Cairns, J. Power Source 165 (2007) 870–873.

[17] J.K. Kim, G. Cheruvally, J.W. Choi, J.H. Ahn, D.S. Choi, C.E. Song, J. Electrochem. Soc. 154 (2007) A839–A843.
[18] S. Yoshihara, H. Isozumi, M. Kasai, H. Yonehara, Y. Ando, K. Oyaizu, H. Nishide, J. Phys. Chem. B 113 (2010) 8335–8340.
[19] M. Suguro, S. Iwasa, Y. Kusachi, Y. Morioka, K. Nakahara, Macromol. Rapid Commun. 28 (2007) 1929–1933.
[20] T. Suga, K. Kasatori, H. Nishide, Polym. Prepr. Jpn. 53 (2) (2004) 4824.
[21] K. Oyaizu, Y. Ando, H. Konishi, H. Nishide, J. Am. Chem. Soc. 130 (2008) 14459–14461.
[22] G. Girishkumar, M. Rettker, R. Underhile, D. Binz, K. Vinodgopal, P. McGinn, P. Kamat, Langmuir 21 (2005) 8487–8494.
[23] M. Yoo, C.W. Frank, S. Mori, S. Yamaguchi, Chem. Mater. 16 (2004) 1945–1953.
[24] R. Ruffo, S.S. Hong, C.K. Chan, R.A. Huggins, Y. Cui, J. Phys. Chem. C 113 (2009) 11390–11398.
[25] C. Hao, L. Ding, X. Zhang, H. Ju, Anal. Chem. 79 (2007) 4442–4447.
[26] K. Xu, Chem. Rev. 104 (2004) 4303–4417.